

## Finite $T$ meson correlations and quark deconfinement

D. Blaschke and G. Bureau

*Fachbereich Physik, Universität Rostock, D-18051 Rostock, Germany*

Yu. L. Kalinovsky

*Laboratory of Computing Techniques and Automation, Joint Institute for Nuclear Research  
141980 Dubna, Russian Federation*

P. Maris and P. C. Tandy

*Center for Nuclear Research, Department of Physics, Kent State University  
Kent, OH 44242, USA*

(December 2, 2024)

### Abstract

A simple confining separable interaction Ansatz for the rainbow-ladder truncated quark Dyson-Schwinger equation and  $\bar{q}q$  Bethe-Salpeter equation is used to study the spatial correlation modes  $\pi$  and  $\rho$  at finite temperature. The model is fixed by  $T = 0$  properties and it implements dynamical chiral symmetry breaking and quark confinement. Transitions for deconfinement ( $T_d$ ) and chiral restoration ( $T_c$ ) are identified. Above and below these transitions we study  $M_\pi(T)$  and  $f_\pi(T)$ , the 3-space transverse and longitudinal masses  $M_\rho^T(T)$  and  $M_\rho^L(T)$ , and the partial widths of the transverse  $\rho$  due to both the electromagnetic decay  $\rho^0 \rightarrow e^+e^-$ , and the strong decay  $\rho \rightarrow \pi\pi$ . The strong width of the  $\rho$  decreases with  $T$ ; it falls to about 50% at  $T_c$  and vanishes some 25 MeV above  $T_c$ , thus leaving the  $\rho$  with only its narrow  $e^+e^-$  width. The simplest version of the model is used to compare the approach to the high  $T$  behavior  $M(T) \rightarrow 2\pi T$  found in lattice QCD simulations.

Pacs Numbers: 11.10.St, 11.10.Wx, 12.38.Mh, 14.40.-n, 24.85.+p

## I. INTRODUCTION

The connection between hot dense hadronic matter and a plasma of quarks and gluons is receiving increased attention with the advent of the relativistic heavy-ion collider (RHIC) at Brookhaven to complement previous investigations at the CERN SPS [1]. The plasma is expected to reveal itself through modified properties of hadronic reactions and their products. The di-lepton spectra has been of considerable interest [2] as a relatively clean signal of how vector meson correlations and their decay channels and widths might be influenced by a hot and dense environment. The question of how a vector meson strong decay, such as  $\rho \rightarrow \pi\pi$ , might respond as the temperature  $T$  or chemical potential  $\mu$  crosses the critical phase boundary for chiral restoration or quark deconfinement requires that this process be studied at the quark-gluon level. To this end it is desirable to be able to describe quark deconfinement and chiral restoration at finite  $T$  and  $\mu$  in a manner that can be extended to a variety of hadronic observables in a rapid and transparent way. The present model provides a simple framework for such investigations.

At  $T = \mu = 0$  significant progress has been made within a continuum approach to modeling non-perturbative QCD based on the truncated Dyson-Schwinger equations (DSEs) [3]. An attractive feature of this approach is that dynamical chiral symmetry breaking and quark confinement can be embodied in the infrared structure of the dressed gluon 2-point function which is constrained by a few chiral meson observables. Recent works have employed the ladder-rainbow truncation of the coupled quark DSE and  $\bar{q}q$  Bethe-Salpeter equation (BSE) to produce successful descriptions of masses and decay constants of the light pseudoscalars  $\pi$  and  $K$  [4] and the vectors  $\rho$ ,  $\phi$ , and  $K^*$  [5]. These works have incorporated the one-loop renormalization group evolution of scale characteristic of QCD. Applications to other hadron observables, including electromagnetic form factors and coupling constants such as  $g_{\rho\pi\pi}$ , have usually required the use of simpler models [6,7].

The finite  $T, \mu$  extension of realistic DSE/BSE models receives extra complications due to the breaking of  $O(4)$  symmetry and the dynamical coupling between Matsubara modes [8,9]. These difficulties are compounded in the subsequent generation of hadronic observables via straightforward adaption of the approach [6] found to be successful at  $T = \mu = 0$ . Studies of hadronic observables at finite  $T, \mu$  in DSE/BSE models have been restricted to simplifications such as extensions of the infrared-dominant (ID) model [10] in which the effective gluon propagator is restricted to an integrable singularity at zero momentum. Nevertheless such a model has proved capable of yielding qualitatively useful information [11–13].

In this work we explore a separable Ansatz that can implement the essential qualitative features of DSE/BSE models at finite temperature. Separable representations have previously been found capable of an efficient modeling of the effective  $\bar{q}q$  interaction in the infrared domain for  $T = 0$  meson observables [14–16]. A previous adaptation to  $T > 0$  was carried out in the absence of a confining mechanism [15]. In the present work, we adapt an existing  $T = \mu = 0$  confining separable interaction Ansatz [16] to make the  $T, \mu > 0$  extension particularly transparent. Some preliminary results have been previously discussed for  $T > 0$  [17] and for  $T, \mu > 0$  [18]. This model implements dynamical chiral symmetry breaking and it preserves the Goldstone theorem in that the generated  $\pi$  is massless in the chiral limit. The confining nature of the quark propagator at  $T = 0$  gives way to a deconfinement transition at a  $T$  value close to that which restores chiral symmetry. The solutions of the

BSE for the  $\pi$  and  $\rho$  modes are particularly simple and are used to study the  $T$ -dependence of the meson masses and decay constants.

In Sec. II the  $T = 0$  separable model is introduced, the DSE solutions for the dressed quark propagator and the BSE solutions for  $\pi$  and  $\rho$  are given, and decay constants are defined. The extension to  $T > 0$  is considered in Sec. III and the spatial  $\pi$  and  $\rho$  modes are discussed. The  $\pi$  mass relation is also considered there with a view towards an evaluation of the performance of this model in respecting chiral symmetry constraints. The widths of the transverse  $\rho$  from  $\rho \rightarrow e^+e^-$  and  $\rho \rightarrow \pi\pi$  are also considered in Sec. III. The behavior of the spatial masses at large  $T$  is considered in Sec. IV where the separable model is compared with the simpler ID model and with results from lattice simulations. A discussion follows in Sec. V.

## II. CONFINING SEPARABLE DYSON-SCHWINGER EQUATION MODEL

In a Euclidean space formulation, with  $\{\gamma_\mu, \gamma_\nu\} = 2\delta_{\mu\nu}$ ,  $\gamma_\mu^\dagger = \gamma_\mu$  and  $a \cdot b = \sum_{i=1}^4 a_i b_i$ , the DSE for the renormalized dressed-quark propagator is

$$S(p)^{-1} = Z_2 i\gamma \cdot p + Z_4 m(\mu) + Z_1 \int_q^\Lambda g^2 D_{\mu\nu}(p-q) \frac{\lambda^a}{2} \gamma_\mu S(q) \Gamma_\nu^a(q; p), \quad (1)$$

where  $D_{\mu\nu}(k)$  is the renormalized dressed-gluon propagator,  $\Gamma_\nu^a(q; p)$  is the renormalized dressed-quark-gluon vertex, and  $\int_q^\Lambda \equiv \int^\Lambda d^4q / (2\pi)^4$  represents a translationally-invariant regularization of the integral, with  $\Lambda$  the regularization mass-scale. The final stage of any calculation is to remove the regularization by taking the limit  $\Lambda \rightarrow \infty$ . The renormalization constants for the quark-gluon-vertex, the quark wave-function, and the mass, namely  $Z_1(\mu^2, \Lambda^2)$ ,  $Z_2(\mu^2, \Lambda^2)$  and  $Z_4(\mu^2, \Lambda^2)$  respectively, depend on the renormalization point and the regularization mass-scale.

In recent years phenomenologically successful models have been developed by truncation of Eq. (1) to the rainbow level  $Z_1 \Gamma_\nu^a(q; p) \rightarrow \gamma_\nu \lambda^a / 2$  together with use of an effective gluon propagator  $D_{\mu\nu}^{\text{eff}}(k)$ . In conjunction with such treatments,  $q\bar{q}$  meson bound states are described by the ladder Bethe-Salpeter equation

$$-\lambda(P^2)\Gamma(p, P) = \frac{4}{3} \int \frac{d^4q}{(2\pi)^4} D_{\mu\nu}^{\text{eff}}(p-q) \gamma_\mu S(q_+) \Gamma(q, P) S(q_-) \gamma_\nu, \quad (2)$$

where  $P$  is the total momentum,  $q_+ = q + \eta P$ ,  $q_- = q + \bar{\eta} P$  and  $\eta = 1 - \bar{\eta}$  is the momentum partitioning parameter. Since this work deals only with mesons of equal mass  $u/d$  quarks, we choose  $\eta = 1/2$ . The meson mass is identified from  $\lambda(P^2 = -M^2) = 1$ . Recent works have employed  $D_{\mu\nu}^{\text{eff}}(k) = \mathcal{G}(k^2) D_{\mu\nu}^{\text{free}}(k)$  where  $D_{\mu\nu}^{\text{free}}(k)$  is the free gluon propagator in Landau gauge. The effective coupling  $\mathcal{G}(k^2)$  is given the one-loop perturbative form of the QCD running coupling in the ultraviolet while the phenomenological infrared form is chosen to reproduce the masses and decay constants of the ground state pseudoscalar mesons  $\pi$  and  $K$  [4]. The masses and decay constants of the vectors  $\rho/\omega$ ,  $K^*$  and  $\phi$  are also well described in such an approach without new parameters [5].

The direct extension of such an approach to accommodate finite temperature [19] and baryon density entails a significant increase in complexity. Furthermore, because of the importance of the pion degree of freedom for the dynamics and thermodynamics of the strongly

interacting system produced in energetic heavy-ion collisions, it is desirable to anticipate the need to consider the extension beyond the zeroth level in meson loops. For this reason we consider here a simple separable interaction model that can reproduce the essential features of the existing ladder-rainbow phenomenology of the coupled DSE/BSE description of low mass  $\pi$  and  $\rho/\omega$  physics. We base our approach on a confining separable model previously found to be successful at  $T = 0$  and defined by [16]  $D_{\mu\nu}^{\text{eff}}(p - q) \rightarrow \delta_{\mu\nu} D(p^2, q^2, p \cdot q)$  with

$$D(p^2, q^2, p \cdot q) = D_0 f_0(p^2) f_0(q^2) + D_1 f_1(p^2) (p \cdot q) f_1(q^2). \quad (3)$$

Here a Feynman-like gauge is chosen for phenomenological simplicity. This is a rank-2 interaction with two strength parameters  $D_0, D_1$ , and corresponding form factors  $f_i(p^2)$ . The choice for these quantities is constrained by consideration of the resulting solution of the DSE for the quark propagator in the rainbow approximation. For the amplitudes defined by  $S(p) = [i\not{p}A(p^2) + B(p^2) + m_0]^{-1}$  this produces

$$B(p^2) = \frac{16}{3} \int \frac{d^4q}{(2\pi)^4} D(p^2, q^2, p \cdot q) \frac{B(q^2) + m_0}{q^2 A^2(q^2) + [B(q^2) + m_0]^2}, \quad (4)$$

$$[A(p^2) - 1] p^2 = \frac{8}{3} \int \frac{d^4q}{(2\pi)^4} D(p^2, q^2, p \cdot q) \frac{(p \cdot q) A(q^2)}{q^2 A^2(q^2) + [B(q^2) + m_0]^2}, \quad (5)$$

where a regularization scale and renormalization constants are absent in anticipation of the interaction form factors being chosen to provide sufficient ultraviolet suppression. In more realistic models [4,5] that include the one-loop renormalization group properties of QCD, the essential features of the low mass meson spectrum are dominated by the infrared dynamics. The present model is aimed only at those essential features.

We note that if terms of higher order in  $p \cdot q$  were to be included in Eq. (3), they would make no contribution to Eqs. (4) and (5) for the DSE solution [16]. The solution for  $B(p^2)$  is determined only by the  $D_0$  term, and the solution for  $A(p^2) - 1$  is determined only by the  $D_1$  term. The solutions are

$$B(p^2) = b f_0(p^2), \quad A(p^2) = 1 + a f_1(p^2), \quad (6)$$

and Eqs. (4) and (5) reduce to nonlinear equations for the constants  $b$  and  $a$ . We choose  $D_i$  and  $f_i(p^2) = \exp(-p^2/\Lambda_i^2)$  to simulate the strength and range of the infrared enhancement of  $A(p^2)$  and  $B(p^2)$  that is evident from more realistic interactions [4,5,16]. If there are no solutions to  $p^2 A^2(p^2) + (B(p^2) + m_0)^2 = 0$  for real  $p^2$  then there is no physical mass pole in the quark propagator, there are no quark production thresholds in hadronic processes, and the quarks are confined [20]. If in the chiral limit ( $m_0 = 0$ ) there is a nontrivial solution for  $B(p^2)$ , then chiral symmetry is dynamical broken. Both phenomena can be implemented in this separable model. With the exponential form for  $f_0(p^2)$ , the confining property can be illustrated easily in the case of a rank-1 separable model where  $D_1 = 0$  and  $A(p^2) = 1$ . In the chiral limit, the model is confining if  $D_0$  is strong enough to make  $b/\Lambda_0 \geq 1/\sqrt{2e}$ . Using  $\Lambda_0 \sim 0.6-0.8$  GeV as a typical range for a quark mass function  $m(p^2) = (B(p^2) + m_0)/A(p^2)$ , confinement will be compatible with  $m(p=0) \geq 0.3$  GeV, an empirically viable value. At finite temperature, the quark mass function strength parameter  $b(T)$  will decrease with  $T$

so that this model can be expected to have a deconfinement transition as well as the chiral restoration transition associated with  $b(T) \rightarrow 0$ .

With the separable interaction of Eq. (3), the allowed form of the solution of Eq. (2) for the pion BS amplitude  $\vec{\tau}\Gamma_\pi(q; P)$  is [16]

$$\Gamma_\pi(q; P) = \gamma_5 \left( iE_\pi(P^2) + \not{P}F_\pi(P^2) \right) f_0(q^2), \quad (7)$$

which contains the two dominant covariants from the set of four general covariants. The  $q$  dependence is described only by the first form factor  $f_0(q^2)$ . The second term  $f_1$  of the interaction can contribute only indirectly via the quark propagators. The  $\pi$  BSE, Eq. (2), becomes a  $2 \times 2$  matrix eigenvalue problem  $\mathcal{K}(P^2)f = \lambda(P^2)f$  where the eigenvector is  $f = (E_\pi, F_\pi)$ . The kernel is

$$\mathcal{K}_{ij}(P^2) = -\frac{4D_0}{3} \text{tr}_s \int \frac{d^4q}{(2\pi)^4} f_0^2(q^2) \left[ \hat{t}_i S(q_+) t_j S(q_-) \right], \quad (8)$$

where the  $\pi$  covariants are  $t = (i\gamma_5, \gamma_5 \not{P})$  and we have also introduced  $\hat{t} = (i\gamma_5, -\gamma_5 \not{P}/2P^2)$ . We note that the separable model produces the same  $q^2$  shape for both amplitudes  $F_\pi$  and  $E_\pi$ ; the shape is that of the quark amplitude  $B(q^2)$ . This is a property shared by the general amplitude  $E_\pi(q; P)$  in the chiral limit, and to a very good approximation away from the chiral limit [4]. However, the general amplitude  $F_\pi(q; P)$  does not have the same shape; it is in fact linked with  $A(q^2) - 1$  through the axial vector Ward-Takahashi identity [21]. One consequence of the AV-WTI that is preserved by the present separable model is Goldstone's theorem; in the chiral limit, whenever a nontrivial DSE solution for  $B(p^2)$  exists, there will be a massless  $\pi$  solution to Eq. (8).

A simple illustrative truncation is obtained by setting  $F_\pi(P^2) = 0$  for then Eq. (8) reduces to an expression for the eigenvalue which is

$$\lambda_\pi(P^2) = \frac{16D_0}{3} \int \frac{d^4q}{(2\pi)^4} f_0^2(q^2) \left[ \left( q^2 - \frac{P^2}{4} \right) \sigma_V^+ \sigma_V^- + \sigma_S^+ \sigma_S^- \right], \quad (9)$$

where the quark propagator amplitudes employed here are defined by  $S(p) = -i\not{p}\sigma_V(p^2) + \sigma_S(p^2)$ . Since  $A = 1$  in rank-1, we omit the amplitude  $F_\pi$  in that case. Thus it is Eq. (9) that we use for the  $\pi$  calculation with a rank-1 interaction.

The vector mesons  $\rho$  and  $\omega$  are degenerate in the ladder approximation. We shall deal with the isovector  $\rho$ . For the BS amplitude  $\vec{\tau}\Gamma_\mu^\rho(q; P)$  there are in general eight transverse covariants [5] and the dominant one is  $\gamma_\mu^T(P) = T_{\mu\nu}(P)\gamma_\nu$  where  $T_{\mu\nu}(P) = \delta_{\mu\nu} - P_\mu P_\nu / P^2$ . The solution of the rank-1 model contains only that term, that is,  $\Gamma_\mu^\rho(q; P) = \gamma_\mu^T(P) f_0(q^2) F_\rho(P^2)$ . The corresponding eigenvalue is given by

$$\lambda_\rho(P^2) = \frac{8D_0}{3} \int \frac{d^4q}{(2\pi)^4} f_0^2(q^2) \left[ \left( q^2 - \frac{P^2}{4} - \frac{2q^2}{3}(1 - z^2) \right) \sigma_V^+ \sigma_V^- + \sigma_S^+ \sigma_S^- \right], \quad (10)$$

where  $z = \hat{q} \cdot \hat{P}$ . For the rank-2 separable interaction, there are two other covariants besides  $\gamma_\mu^T$  that will appear in the solution of the BSE [16]. However it has been found in such a model that these subleading vector covariants make only a few percent contribution to

the vector mass [16] and the associated  $g_{\rho\pi\pi}$  [7]. In this present work we will ignore the subdominant covariants and employ  $\gamma_\mu^T$  as the only covariant for the vector meson. The differences in the vector mass obtained from Eq. (10) in rank-1 and rank-2 will be due to differences in the quark propagator in each case.

The normalization condition for the  $\pi$  BS amplitude can be expressed as

$$2P_\mu = \frac{\partial}{\partial P_\mu} 2N_c \text{tr}_s \int \frac{d^4q}{(2\pi)^4} \bar{\Gamma}_\pi(q; -K) S(q_+) \Gamma_\pi(q; K) S(q_-) \Big|_{P^2=K^2=-M_\pi^2}. \quad (11)$$

This produces  $E_\pi(P^2 = -M_\pi^2) f_0(q^2) = B(q^2)/N_\pi$ . If the axial vector Ward-Takahashi identity is satisfied, the normalization constant defined this way will have the chiral limit value  $N_\pi^0 = f_\pi^0$  with  $f_\pi^0$  being the chiral limit weak decay constant [21]. The normalization for the vector meson is set by [5]

$$2P_\mu = \frac{\partial}{\partial P_\mu} \frac{2N_c}{3} \text{tr}_s \int \frac{d^4q}{(2\pi)^4} \bar{\Gamma}_\nu(q; -K) S(q_+) \Gamma_\nu(q; K) S(q_-) \Big|_{P^2=K^2=-M_V^2}. \quad (12)$$

Here  $\bar{\Gamma}(q; K)$  is the charge conjugate amplitude  $[\mathcal{C}^{-1}\Gamma(-q, K)\mathcal{C}]^t$  where  $\mathcal{C} = \gamma_2\gamma_4$  and  $t$  denotes matrix transpose. The result is  $\bar{\Gamma}(q; K) = C\Gamma(q; K)$  with charge parities  $C_\pi = +1$  and  $C_\rho = -1$ .

The pion decay constant  $f_\pi$ , defined by

$$f_\pi P_\mu \delta_{ij} = \langle 0 | \bar{q} \frac{\tau_i}{2} \gamma_\mu \gamma_5 q | \pi_j(P) \rangle, \quad (13)$$

can be expressed as the loop integral

$$f_\pi P_\mu = N_c \text{tr}_s \int \frac{d^4q}{(2\pi)^4} \gamma_5 \gamma_\mu S(q_+) \Gamma_\pi(q; P) S(q_-). \quad (14)$$

For the vector meson, the electromagnetic decay mediated by a photon (e.g.  $\rho^0, \omega$ ) and the leptonic decay mediated by a W-boson (e.g.  $\rho^\pm$ ) are described by the vector decay constant  $f_V$ . In the normalization for the vector meson used here, we have [5,22]

$$f_\rho M_\rho T_{\mu\nu}(P) = \langle 0 | \bar{d} \gamma_\mu u | \rho_\nu^+(P) \rangle. \quad (15)$$

This produces the loop integral

$$\frac{M_\rho^2}{g_\rho} = \frac{f_\rho M_\rho}{\sqrt{2}} = \frac{N_c}{3} \text{tr}_s \int \frac{d^4q}{(2\pi)^4} \gamma_\mu S(q_+) \Gamma_\mu(q; P) S(q_-), \quad (16)$$

where  $g_\rho$  is the coupling constant conventionally used to describe the electromagnetic decay of the  $\rho^0$ . Eqs. (14) and (16) are the exact expressions for  $f_\pi$  and  $f_\rho$  except for the absence of regulation and the multiplicative renormalization constant  $Z_2(\Lambda, \mu)$ . The decay constants thus test the quality of the infrared behavior of the quark propagator and the BS amplitudes.

In Table I the results for the ground state  $\pi$  and  $\rho/\omega$  mesons as well as related quantities are shown for both rank-1 and rank-2 versions of the model along with the values of the employed parameters. We consider the experimental  $\omega$  mass to be the appropriate value for

comparision with the vector result in ladder approximation in order to allow for subsequent preferential lowering of  $M_\rho$  due to pion loop dressing [23]. The range parameter  $\Lambda_0$  is used to set the mass scale to reproduce the experimental  $M_\omega$  for rank-1 and  $f_\pi$  for rank-2. The obtained dynamical quark mass function at  $p^2 = 0$  is  $m(p^2 = 0) = 0.685$  GeV for rank-1. This is about 40% larger than what is found in realistic DSE solutions [4,5]. For rank-2 we obtain  $A(p^2 = 0) = 1.94$  and  $m(p^2 = 0) = 0.405$  GeV which is more characteristic. In both cases the dressed quark propagator is confining.

As a test of the quality of a  $\bar{q}q$  model of the pion, one may consider the chiral symmetry constraint embodied in the axial vector Ward-Takahashi identity (AV-WTI)

$$-iP_\mu \Gamma_{5\mu}(q; P) = S^{-1}(q_+) \gamma_5 + \gamma_5 S^{-1}(q_-) - 2m_0 \Gamma_5(q; P), \quad (17)$$

where  $\vec{\tau}/2\Gamma_{5\mu}$  is the isovector axial vector vertex and  $\vec{\tau}/2\Gamma_5$  is the isovector pseudoscalar vertex. Both vertex functions  $\Gamma_{5\mu}$  and  $\Gamma_5$  are characterized by  $\gamma_5 \gamma_\mu + \tilde{\Gamma}_{5\mu}(q; P)$  and  $\gamma_5 + \tilde{\Gamma}_5(q; P)$  respectively. With the ladder approximation, and with the separable model of the Bethe-Salpeter kernel, the amplitudes  $\tilde{\Gamma}(q; P)$  have the same general form as the corresponding meson solutions of the homogeneous equation. In particular,  $\tilde{\Gamma}_5(q; P) = f_0(q^2) \tilde{F}(P)$  and  $\tilde{\Gamma}_{5\mu}(q; P) = f_0(q^2) \tilde{F}_\mu^0(q; P) + f_1(q^2) \tilde{F}_\mu^1(q; P)$ , where  $\tilde{F}(P)$  and  $\tilde{F}_\mu^i(q; P)$  are Dirac matrices and the latter is at most linear in  $q$ . Since  $S^{-1}(q_\pm)$  does not separate this way in its  $q$  and  $P$  dependence, Eq. (17) cannot be satisfied within a separable model.

There are momentum independent relations between pion quantities that follow from Eq. (17) that might be satisfied to some satisfactory level within a separable model. One such relation is  $N_\pi/f_\pi = 1$  [21]. The rank-1 model produces  $N_\pi/f_\pi = 0.987$  while the rank-2 model produces  $N_\pi/f_\pi = 0.74$ . The agreement in the former case simply reflects the observation [3] that any model that enforces  $A(p^2) = 1$  will preserve this relation. In the more general case where  $A(p^2) \neq 1$ , the equality of  $N_\pi$  and  $f_\pi$  relies on use of the general representation for the pion BS amplitude. The larger deviation seen here in rank-2 is a realistic measure of the limited ability of a separable model in representing the pion BS amplitude (Eq. (7)). In Sec. III, an examination of the  $T$ -dependence of the exact  $\pi$  mass relation will reveal deviations very similar to the above  $N_\pi/f_\pi$  values.

### III. FINITE TEMPERATURE EXTENSION

The extension of the separable model studies of the previous section to  $T \neq 0$  is systematically accomplished by transcription of the Euclidean quark 4-momentum via  $q \rightarrow q_n = (\omega_n, \vec{q})$ , where  $\omega_n = (2n + 1)\pi T$  are the discrete Matsubara frequencies. We assume that  $T$ -dependence enters only through those quantities that have a  $p^2$ -dependence at  $T = 0$ . The model interaction will thus weaken with  $T$  through the dependence of the form factors upon  $\omega_n$ . In this approach, there are no new parameters and we wish to study the  $T$ -dependence of the quark propagator and meson properties produced this way. In particular, the quark dynamical mass will decrease with  $T$  and we are interested in the behavior of the  $\pi$  and  $\rho$  meson modes and decay constants with the resulting deconfinement and chiral restoration.

The result of the DSE solution for the dressed quark propagator can be expressed as

$$S^{-1}(p_n, T) = i\vec{\gamma} \cdot \vec{p} A(p_n^2, T) + i\gamma_4 \omega_n C(p_n^2, T) + B(p_n^2, T) + m_0, \quad (18)$$

where  $p_n^2 = \omega_n^2 + \vec{p}^2$  and there are now three amplitudes due to the loss of  $O(4)$  symmetry. They have the form  $B = b(T)f_0(p_n^2)$ ,  $A = 1 + a(T)f_1(p_n^2)$ , and  $C = 1 + c(T)f_1(p_n^2)$  and the DSE becomes a set of three non-linear equations for  $b(T)$ ,  $a(T)$  and  $c(T)$ . The explicit form is

$$a(T) = \frac{8D_1}{9} T \sum_n \int \frac{d^3p}{(2\pi)^3} f_1(p_n^2) \vec{p}^2 [1 + a(T)f_1(p_n^2)] d^{-1}(p_n^2, T), \quad (19)$$

$$c(T) = \frac{8D_1}{3} T \sum_n \int \frac{d^3p}{(2\pi)^3} f_1(p_n^2) \omega_n^2 [1 + c(T)f_1(p_n^2)] d^{-1}(p_n^2, T), \quad (20)$$

$$b(T) = \frac{16D_0}{3} T \sum_n \int \frac{d^3p}{(2\pi)^3} f_0(p_n^2) [m_0 + b(T)f_0(p_n^2)] d^{-1}(p_n^2, T), \quad (21)$$

where  $d(p_n^2, T)$  is given by

$$d(p_n^2, T) = \vec{p}^2 A^2(p_n^2, T) + \omega_n^2 C^2(p_n^2, T) + [m_0 + B(p_n^2, T)]^2. \quad (22)$$

It is also useful to introduce the equivalent representation

$$S(p_n, T) = -i\vec{\gamma} \cdot \vec{p} \sigma_A(p_n^2, T) - i\gamma_4 \omega_n \sigma_C(p_n^2, T) + \sigma_B(p_n^2, T), \quad (23)$$

where  $\sigma_A = A/d$ ,  $\sigma_C = C/d$  and  $\sigma_B = (B + m_0)/d$ .

The  $T$ -dependence of the solutions at  $p^2 = 0$  for the rank-2 model is displayed in Fig. 1. The results shown are for the lowest Matsubara mode ( $n = 0$ ) which provides the leading behavior as  $T$  is increased. The chiral restoration critical temperature  $T_c$  is identified from the vanishing of the chiral limit amplitude  $B_0(p = 0, T)$  as shown. We find  $T_c = 121$  MeV for the rank-2 model. Below  $T_c$ ,  $A$  and  $C$  are relatively constant,  $O(4)$  symmetry is approximately manifest, and the main effect is an almost constant quark wave function renormalization via  $1/C$ ; the central feature shared by both rank-1 and rank-2 models is a rapidly decreasing mass function. Above  $T_c$ , there remains a significant temperature range where the self-interaction effects are strong, both  $A$  and  $C$  are considerably enhanced above their perturbative values, and the breaking of  $O(4)$  symmetry is manifest. Such features have been observed in other DSE studies that employ different interaction models. These include an infrared dominant model represented by a momentum space delta function [11] and a study that supplemented that model by a finite range tail [8]. These realistic features are also captured by the separable model if the rank-2 form is used. The rank-1 model has  $A = C = 1$  for all  $T$  and the behavior of  $B(p = 0, T)$  is similar to that in Fig. 1 except  $T_c = 146$  MeV is obtained.

The order parameter for chiral restoration, the chiral quark condensate, can be obtained from the chiral quark propagator as  $\langle \bar{q}q \rangle^0 = -N_c \text{tr}_s S_0(x, x)$ . Here this produces

$$\langle \bar{q}q \rangle^0 = -4N_c T \sum_n \int \frac{d^3p}{(2\pi)^3} \frac{b_0(T) f_0(p_n^2)}{d_0(p_n^2, T)}, \quad (24)$$

where  $b_0$  and  $d_0$  are obtained from the chiral limit solution of the DSE. Both  $b_0(T)$  and  $\langle \bar{q}q \rangle^0$  vanish sharply as  $(1 - T/T_c)^\beta$  with the critical exponent having the mean field value  $\beta = 1/2$  in agreement with other rainbow DSE studies [24].

The deconfinement temperature  $T_d$  is found by a search for a propagator pole (a zero of the function  $d(p_0^2, T)$ ) on the real  $\vec{p}^2$  axis. We find  $T_d = T_c = 146$  MeV for the rank-1 model and  $T_d = 105$  MeV for the rank-2 model. We have found that only about 15% variation in these transition temperatures can be achieved by variation of the model parameters while retaining a reasonable description of the observables shown in Table I. Since all dynamical information concerning the rank-1 model is contained in one function  $B(p_n^2, T)$  generated by one form factor, the result  $T_d = T_c$  is not surprising. For rank-2, the dynamical information is generated from two form factors and it is possible that dynamical correlations between the three functions  $A, B, C$  are reduced by the separability feature. The observation in the present rank-2 model that deconfinement occurs at a  $T_d$  that is 16 MeV less than  $T_c$  may be due to this or it may be a more general phenomenon.

### A. Spatial $\pi$ correlations at $T \neq 0$

At  $T = 0$  the mass-shell condition for a meson as a  $\bar{q}q$  bound state of the BSE is equivalent to the appearance of a pole in the  $\bar{q}q$  scattering amplitude as a function of  $P^2$ , where the total 4-momentum is  $P = (\Omega_m, \vec{P})$ . At  $T \neq 0$  the  $O(4)$  symmetry is broken, and the dependence of quark propagator amplitudes, and hence BS amplitudes, upon  $\Omega$  and  $\vec{P}$  is no longer in terms of the combination  $\Omega^2 + \vec{P}^2$ . The eigenvalues of the meson BSE become  $\lambda(P^2) \rightarrow \tilde{\lambda}(\Omega^2, \vec{P}^2; T)$ . The temporal meson modes identified by zeros of  $1 - \tilde{\lambda}(\Omega_m^2, 0; T)$  will be different in general from the spatial modes identified by zeros of  $1 - \tilde{\lambda}(0, \vec{P}^2; T)$ . At low enough  $T$  where the  $O(4)$  symmetry is not strongly broken, one expects the temporal and spatial modes to be degenerate. In this work we explore the  $T$ -dependence of the lowest spatial masses in the  $\pi$  and  $\rho$  channels.

In the  $\pi$  channel, the correlator  $\Pi(x) = \langle T J_{ps}(x) J_{ps}(0) \rangle$  of two currents  $J_{ps}(x) = \bar{q}(x)\gamma_5 q(x)$ , after transformation to momentum space and extension to  $T > 0$  via the Matsubara formalism, can be expressed as

$$\Pi(\Omega^2, \vec{P}^2) = N_c T \sum_n \text{tr}_s \int \frac{d^3 q}{(2\pi)^3} \gamma_5 S(q_{n+}) \Gamma_{ps}(q_n; \Omega, \vec{P}) S(q_{n-}), \quad (25)$$

where  $q_{n\pm} = q_n \pm P/2$  and  $\Gamma_{ps}$  is the pseudoscalar vertex which satisfies the inhomogeneous version of the pion BSE. The quark propagators appearing are dressed according to solution of the DSE. When the ladder approximation is employed for  $\Gamma_{ps}$ , along with the present separable approximation to the BSE kernel, the correlation function can be expressed as

$$\Pi(\Omega^2, \vec{P}^2) = \Pi^{(0)}(\Omega^2, \vec{P}^2) - \frac{4D_0}{3} N_c \frac{L_i(\Omega^2, \vec{P}^2) \hat{L}_j(\Omega^2, \vec{P}^2)}{\delta_{ij} - \mathcal{K}_{ij}(\Omega^2, \vec{P}^2)}. \quad (26)$$

Here  $\Pi^{(0)}$  is the contribution to Eq. (25) arising from the zeroth order contribution ( $\gamma_5$ ) to the pseudoscalar vertex  $\Gamma_{ps}$ . The numerator of the second term of Eq. (26) is the contribution that is first order in the interaction, and because of the separable form, it factorizes. The

denominator involves the  $T > 0$  extension of kernel of the  $\pi$  separable BSE given previously in Eq. (8). The loop integrals for the numerator are given by

$$L_i(\Omega^2, \vec{P}^2) = T \sum_n \text{tr}_s \int \frac{d^3 q}{(2\pi)^3} f_0(q_n^2) \gamma_5 S(q_{n+}) t_i S(q_{n-}), \quad (27)$$

and

$$\hat{L}_j(\Omega^2, \vec{P}^2) = T \sum_n \text{tr}_s \int \frac{d^3 q}{(2\pi)^3} f_0(q_n^2) \hat{t}_j S(q_{n+}) \gamma_5 S(q_{n-}). \quad (28)$$

With an eigenvector representation of the BSE kernel  $\mathcal{K}$ , the denominator in Eq. (26) becomes  $1 - \tilde{\lambda}_\pi(\Omega^2, \vec{P}^2; T)$ . There is a pole in the correlator associated with the spatial mode solution to the homogeneous BSE identified from

$$1 - \tilde{\lambda}_\pi(0, \vec{P}^2; T) = Z_\pi^{-1}(\vec{P}^2, T)[\vec{P}^2 + M_\pi^2(T)] = 0. \quad (29)$$

The masses so identified are spatial screening masses of the lowest mode associated with the 3-space asymptotic behavior  $\Pi(x) \sim \exp(-Mx)$ . The identification of spatial masses by location of a pole is related by Fourier transformation to the large source separation method used in lattice QCD.

The general form of the finite  $T$  pion BS amplitude allowed by the separable model is

$$\Gamma_\pi(q_n; P_m) = \gamma_5 \left( iE_\pi(P_m^2) + \gamma_4 \Omega_m \tilde{F}_\pi(P_m^2) + \vec{\gamma} \cdot \vec{P} F_\pi(P_m^2) \right) f_0(q_n^2). \quad (30)$$

The separable BSE becomes a  $3 \times 3$  matrix eigenvalue problem with a kernel that is a generalization of Eq. (8). In the limit  $\Omega_m \rightarrow 0$ , as is required for the spatial mode of interest here, the amplitude  $\hat{F}_\pi = \Omega_m \tilde{F}_\pi$  associated with the lowest mode is trivially zero. The obtained  $T$ -dependence of the properly normalized  $\pi$  BS amplitudes  $E_\pi f_0(q_n^2)$  and  $F_\pi f_0(q_n^2)$  at  $\vec{q} = 0$  and for the lowest Matsubara mode  $n = 0$  is displayed in Fig. 2 for the rank-2 model. The  $T_c$  marked there is the rank-2 value. The rank-1 amplitude is also displayed for comparison. The  $\gamma_5$  amplitude  $E_\pi$  is some 50% larger than the pseudovector amplitude  $F_\pi$ ; the latter decreases rapidly to zero above the transition. In the chiral limit, it vanishes identically at the transition. The result for the  $\pi$  mass is displayed in Fig. 3 for rank-1 and in Fig. 4 for rank-2. In both models,  $M_\pi(T)$  is seen to be only weakly  $T$ -dependent until near  $T_c$  where a sharp rise begins. This behavior of  $M_\pi(T)$  has also been observed within studies of approximate mass relations for the pion based on dynamical chiral symmetry breaking and restoration in DSE models of the quark propagator [8]. The rise near  $T_c$  can be understood from the behavior of the exact pion mass relation as  $T_c$  is approached [24]. In a more direct way, a recent study of the ladder-rainbow truncation of the DSE/BSE complex with a realistic non-separable interaction consistent with the one-loop renormalization group properties of QCD shows the same qualitative behavior [19].

## B. Chiral symmetry and $\pi$ mass relation

To explore the extent to which the model respects the detailed constraints from chiral symmetry, we investigate the exact QCD pseudoscalar mass relation [21] which, after extension to the spatial mode at  $T > 0$ , is

$$M_\pi^2(T) f_\pi(T) = 2m_0 r_P(T). \quad (31)$$

Here  $r_P$ , the residue at the pion pole in the pseudoscalar vertex, is given by the pseudoscalar projection of the pion wavefunction onto zero quark-antiquark separation, that is

$$ir_P(T) = N_c T \sum_n \text{tr}_s \int \frac{d^3q}{(2\pi)^3} \gamma_5 S(q_n + \frac{\vec{P}}{2}) \Gamma_\pi(q_n; \vec{P}) S(q_n - \frac{\vec{P}}{2}). \quad (32)$$

The generalization of Eq. (14) for  $f_\pi$  to finite temperature in the case of the spatial pion mode is

$$P_i f_\pi(T) = N_c T \sum_n \text{tr}_s \int \frac{d^3q}{(2\pi)^3} \gamma_5 \gamma_i S(q_n + \frac{\vec{P}}{2}) \Gamma_\pi(q_n; \vec{P}) S(q_n - \frac{\vec{P}}{2}). \quad (33)$$

Eqs. (32) and (33) are exact expressions for  $r_P(T)$  and  $f_\pi(T)$  except that regulation and multiplicative renormalization constants  $Z_4$  and  $Z_2$  respectively are not needed for this separable model. The relation in Eq. (31) is a consequence of the pion pole structure of the isovector axial Ward identity which links the quark propagator, the pseudoscalar vertex and the axial vector vertex [21]. In the chiral limit,  $r_P \rightarrow -\langle \bar{q}q \rangle^0 / f_\pi^0$  and Eq.(31), for small mass, produces the Gell-Mann–Oakes–Renner (GMOR) relation. The exact mass relation, Eq. (31), can only be satisfied approximately when the various quantities are obtained in a manner that does not preserve axial Ward identity. The error can be used to assess the reliability of the present approach to modeling the behavior of the pion spatial mode as the temperature is varied.

Our findings in the case of the rank-1 model are displayed in Fig. 3. There the solid line represents  $r_P(T)$  calculated from the quark loop integral in Eq. (32); the dotted line represents  $r_P$  constructed from the other quantities in Eq. (31). The rank-1 model obeys this exact QCD mass relation to better than 1% for temperatures up to and beyond the restoration of chiral symmetry. This corresponds to the agreement between  $N_\pi$  and  $f_\pi$  to within 1% at  $T = 0$  as noted in Sec. II and is due to the special case  $A = C = 1$ . We have also investigated the (approximate) GMOR relation within the present model. The quantity  $-\langle \bar{q}q \rangle^0 / N_\pi^0$ , displayed in Fig. 3, is the chiral limit of  $r_P$  in this model. If all covariants for the pion were retained and the axial vector Ward identity were obeyed, one would have  $N_\pi^0 = f_\pi^0$  in the chiral limit [21]. If the GMOR relation were exactly obeyed, the long-dashed line representing  $\langle \bar{q}q \rangle^0 / N_\pi^0$  would coincide with the dotted line representing  $M_\pi^2 f_\pi / 2m_0$ . The results in Fig. 3 indicate that the GMOR relation is violated by about 5% in the rank-1 separable model and that it differs from the model-consistent exact mass relation by about the same amount. These features are temperature-independent until about  $0.9 T_c$ . This is consistent with an earlier study of low energy theorems at  $T > 0$  within a three-space, non-confining separable interaction model [25].

It should be noted that  $f_\pi^0$ ,  $N_\pi^0$  and  $\langle \bar{q}q \rangle^0$  are equivalent order parameters for the critical behavior near  $T_c$  and have weak  $T$ -dependence below  $T_c$ . A consequence is that  $M_\pi^2 f_\pi$ ,  $r_P$  and  $\langle \bar{q}q \rangle^0 / N_\pi^0$  are almost  $T$ -independent and so are the estimated errors for the two mass relations linking these quantities. We have employed the physical  $f_\pi$  defined at non-zero current quark mass, and this does not vanish at  $T_c$  but continuously decreases.

In Fig. 4, we display the same comparison for the rank-2 model. In this case the exact mass relation is violated by about 25% while the GMOR relation is violated by about 45%.

Without the constraint  $A = C = 1$ , the quark propagator has a more realistic representation and the limitations in the separable model representation of the pion BS amplitude are what is being revealed here. Without a separable approximation, the ladder-rainbow truncation of the DSE/BSE system preserves the exact pion mass relation, Eq. (31), at  $T > 0$  as recently demonstrated [19].

### C. Spatial $\rho$ correlations at $T \neq 0$

The  $T = 0$  transverse vector meson, that we have described by the covariant  $\gamma_\mu^T$ , splits for  $T > 0$  into 3-space longitudinal and transverse modes. For the spatial modes characterized by  $P = (0, \vec{P})$  the BS amplitudes are

$$\Gamma_\mu^{\rho(L)}(q_n; \vec{P}) = \delta_{\mu 4} \gamma_4 f_0(q_n^2) F_{\rho(L)}(\vec{P}^2), \quad (34)$$

and

$$\Gamma_i^{\rho(T)}(q_n; \vec{P}) = \left( \gamma_i - \frac{P_i \vec{P} \cdot \vec{\gamma}}{\vec{P}^2} \right) f_0(q_n^2) F_{\rho(T)}(\vec{P}^2). \quad (35)$$

The  $T$ -dependence of the corresponding masses is displayed in Fig. 5 for the rank-2 model. These modes are effectively degenerate and  $T$ -independent until about  $T_c/2$  where the breaking of  $O(4)$  invariance becomes significant. The qualitative features  $M_\rho^L(T) > M_\rho^T(T)$  and  $M_\rho^T(T) \approx \text{const}$  for  $T < T_c$  seen here in the present context of a finite range interaction have previously been noted within the limiting case of the zero momentum range (infrared dominant) model [12]. This latter model was not applied for  $T > T_c$ . In the present study, the longitudinal mode become unstable to  $\bar{q}q$  dissociation for  $T \sim 180$  MeV at which point the present investigation is discontinued. The transverse mode continues to be below the spatial  $\bar{q}q$  threshold for the temperature range displayed.

The electromagnetic decay constant  $g_\rho(T)$  that describes the coupling of the transverse  $\rho^0$  (with  $\Omega_m = 0$ ) to the photon is given by a straightforward extension of the  $T = 0$  expression in Eq. (16), that is

$$\frac{M_\rho^{T^2}(T)}{g_\rho(T)} = \frac{f_\rho(T) M_\rho^T(T)}{\sqrt{2}} = \frac{N_c}{2} T \sum_n \text{tr}_s \int \frac{d^3 q}{(2\pi)^3} \gamma_i S(q_n + \frac{\vec{P}}{2}) \Gamma_1^{\rho(T)}(q_n; \vec{P}) S(q_n - \frac{\vec{P}}{2}), \quad (36)$$

where  $f_\rho(T)$  is the corresponding vector decay constant. The electromagnetic decay width of the transverse  $\rho$  mode is calculated from

$$\Gamma_{\rho^0 \rightarrow e^+ e^-}(T) = \frac{4\pi \alpha^2 M_\rho^T(T)}{3 g_\rho^2(T)}. \quad (37)$$

At  $T = 0$  the experimental value is  $\Gamma_{\rho^0 \rightarrow e^+ e^-}(0) = 6.77$  keV corresponding to the value  $g_\rho^{\text{expt}}(0) = 5.03$ . The  $T = 0$  width obtained from the rank-2 separable model is 4.29 keV ( $g_\rho(0) = 6.38$ ), while with rank-1 the result is 6.88 keV ( $g_\rho(0) = 5.04$ ). These results are summarized in Table I where the corresponding values for  $f_\rho(0)$  are also given. Our result

for the  $T$  dependence of the electromagnetic width of the 3-space transverse  $\rho$  mode is displayed in Fig. 6 while the corresponding coupling constant  $g_\rho(T)$  is displayed in Fig. 7. It is found that  $\Gamma_{\rho \rightarrow e^+e^-}(T)$  remains within 20% of the  $T = 0$  value even for a significant temperature range above  $T_c$ . An increase in  $\Gamma_{\rho \rightarrow e^+e^-}(T)$  has been explored empirically in connection with possible medium effects on the heavy-ion dilepton spectrum [26]. The present study does not support a significant change.

However the present study does support a significant suppression of the strong decay of the  $\rho$ . The impulse approximation for the  $\rho\pi\pi$  vertex, after extension to  $T > 0$  for spatial modes characterized by  $Q = (0, \vec{Q})$  for the  $\rho$  and  $2P = (0, 2\vec{P})$  for the total  $\pi\pi$  momentum, takes the form

$$\begin{aligned} \Lambda_\nu(P, Q) &= P_\nu g_{\rho\pi\pi}(T) \\ &= -2N_c T \sum_n \text{tr}_s \int \frac{d^3q}{(2\pi)^3} \Gamma_\pi(k_{n+}; -\vec{P}_+) S(q_{n+-}) \Gamma_\nu^{\rho(T/L)}(q_{n+}; \vec{Q}) S(q_{n++}) \Gamma_\pi(k_{n-}; \vec{P}_-) S(q_{n-}), \end{aligned} \quad (38)$$

where  $\vec{P}_\pm = \vec{P} \pm \vec{Q}/2$ ,  $q_{n\pm} = q_n \pm \vec{P}/2$ ,  $q_{n\pm\pm} = q_{n\pm} \pm \vec{Q}/2$  and  $k_{n\pm} = q_n \pm \vec{Q}/4$ . The quark loop momentum is  $q_n = (\omega_n, \vec{q})$ . The  $\Gamma_\pi(k_n; P)$  is the pion BS amplitude in Dirac spin space corresponding to relative  $\bar{q}q$  momentum  $k_n$  (we choose equal partitioning) and pion momentum  $P$  entering the loop. The mass-shell conditions imposed are  $\vec{Q}^2 = -M_\rho^2$  and  $\vec{P}_\pm^2 = -M_\pi^2$ . Use of Eq. (34) immediately shows that the longitudinal  $\rho$  mode cannot couple to  $\pi\pi$ . The temperature evolution of the  $\pi\pi$  decay of the transverse  $\rho$  is influenced strongly by the different  $T$ -dependence of  $M_\pi(T)$  and  $M_\rho^T(T)$ . As displayed in Fig. 5,  $2M_\pi(T)$  for  $T > T_c$  increases faster than does  $M_\rho^T(T)$  until at  $T = 1.17 T_c$  we find  $M_\rho^T = 2M_\pi$  after which the strong decay  $\rho^T \rightarrow \pi\pi$  is closed because there is no available phase space. This occurs at  $T = 1.11 T_c$  in the rank-1 model.

The produced  $\rho \rightarrow \pi\pi$  decay width is given by

$$\Gamma_{\rho \rightarrow \pi\pi}(T) = \frac{g_{\rho\pi\pi}^2(T) m_\rho^T(T)}{4\pi} \frac{m_\rho^T(T)}{12} \left[ 1 - \frac{4m_\pi^2(T)}{m_\rho^T(T)} \right]^{3/2}. \quad (39)$$

The experimental value at  $T = 0$  is 151 MeV. We obtain 221 MeV with the rank-2 model and 137 MeV with rank-1. Our rank-2 result for the  $T$  dependence of the  $\pi\pi$  width of the  $\rho^T$  mode is displayed in Fig. 6; the corresponding coupling constant  $g_{\rho\pi\pi}(T)$  is displayed in Fig. 7. Beyond  $T = 1.17 T_c$  (142 MeV) the  $\pi\pi$  decay channel is phase-space blocked, the corresponding width vanishes and the coupling constant is not relevant. For a significant domain of higher  $T$ , Fig. 6 emphasizes that the transverse  $\rho$  spatial mode can only decay via the electroweak mechanism yielding lepton pairs. The total  $\rho^T$  width of 151 MeV at  $T = 0$  decreases by about 50% at  $T = T_c$  and drops sharply to the electromagnetic value of about 6 keV by  $T = 1.17 T_c$ . This narrowing of the decay width of the intrinsic vector meson mode in the heat bath contrasts with the collisional broadening effect [2] from the many-body environment.

#### IV. BEHAVIOR AT LARGE $T$

The quark deconfinement point  $T_d$  and the chiral restoration point  $T_c$  are generally expected to be identical or nearly so [27]. The present separable model produces  $T_d = T_c$  in rank-1 and  $T_d = 0.72 T_c$  in rank-2. It might be expected therefore that above  $T_c$  meson modes should dissolve in favor of a gas of essentially massless quarks. However for a significant temperature range above  $T_c$ , the spatial  $\pi$  and  $\rho$  modes studied here continue to be stable against  $\bar{q}q$  dissociation and do not dissolve into a free quark gas. This situation is clearest for the simpler rank-1 separable interaction. The results for  $M_\pi(T)$  and  $M_\rho^T(T)$  obtained from the eigenmass condition  $\lambda(-M^2) = 1$  are displayed in Fig. 8 along with the quark dynamical mass function at  $p = 0$ . The masses of both spatial meson modes approach the asymptotic behavior  $2\pi T$  from below. This asymptotic behavior has been discussed previously [28] and is observed in lattice simulations [27,28].

The manner in which the  $2\pi T$  behavior at large  $T$  emerges from the present description is illustrated well by the rank-1 model. For  $T > T_c$ , the dynamically generated mass function of the quarks is essentially negligible, and only the Dirac vector part of the quark propagator is relevant. For the spatial  $\pi$  mode characterized by  $P = (0, \vec{P})$ , the loop integral for the ‘‘polarization’’ function or BSE eigenvalue  $\lambda_\pi(\vec{P}^2)$ , given by Eq. (9), yields at large  $T$

$$\lambda_\pi(\vec{P}^2) \approx \frac{16D_0}{3} T \int \frac{d^3q}{(2\pi)^3} f_0^2(\pi^2 T^2 + \vec{q}^2) \frac{\pi^2 T^2 + \vec{q}^2 - \frac{P^2}{4}}{[\pi^2 T^2 + (\vec{q} + \vec{P}/2)^2][\pi^2 T^2 + (\vec{q} - \vec{P}/2)^2]}, \quad (40)$$

where only the dominant zeroth Matsubara mode has been retained. For  $T \gg \Lambda_0/\pi$ , with  $\Lambda_0$  being the range of the interaction form factor  $f_0$ , only small  $q$  is relevant and the position of the lowest singularity as a function of  $\vec{P}^2 < 0$  approaches  $2\pi T$ . The higher the temperature, the more  $\lambda_\pi(\vec{P}^2)$  is suppressed except near the singularity. The value  $\lambda_\pi(-M^2) = 1$  must be encountered before the divergence and thus  $M_\pi(T) \sim 2\pi T - \Delta_\pi(T)$  where  $\Delta_\pi$  is a positive mass defect that will typically decrease with  $T$ . Thus the spatial meson mass or screening mass will approach the thermal mass of a pair of massless fermions from below. Since the range of the interaction is immaterial to this analysis, it is not surprising that the asymptotic  $T$  behavior is the same as that obtained from the pseudoscalar correlator within the Nambu–Jona-Lasinio model [29].

The same qualitative behavior at large  $T$  can be seen in a semi-analytic way by considering the extension to  $T > 0$  of the infrared dominant model introduced at  $T = 0$  by Munczek and Nemirovsky [10]. For the Feynman-like gauge used in the present study, the effective interaction of this model is specified by

$$D(p - q) \rightarrow (2\pi)^4 \frac{3\eta^2}{16} \delta^4(p - q), \quad (41)$$

which is to be used in the DSEs given in Eqs. (4) and (5) and also in the BSE given in Eq. (2). The results are unchanged when Landau gauge is used if Eq. (41) is scaled up by  $4/3$ . In the chiral limit, closed form expressions exist for the resulting quark propagator amplitudes and for the ladder BSE eigenvalues  $\lambda(P^2)$  in the pseudoscalar and vector channels of interest here. The chiral limit DSE solution is of the general form given in Eq. (23) with

$$\sigma_A(p^2) = \sigma_C(p^2) = \begin{cases} \frac{2}{\eta^2}, & p^2 \leq \frac{\eta^2}{4} \\ \frac{2}{p^2} \left[ 1 + \left( 1 + \frac{2\eta^2}{p^2} \right)^{\frac{1}{2}} \right]^{-1}, & p^2 \geq \frac{\eta^2}{4} \end{cases}$$

$$\sigma_B(p^2) = \begin{cases} \frac{1}{\eta^2}(\eta^2 - 4p^2)^{\frac{1}{2}}, & p^2 \leq \frac{\eta^2}{4} \\ 0, & p^2 \geq \frac{\eta^2}{4} \end{cases}. \quad (42)$$

Here the quark mass function is  $m^2(p^2) = \eta^2/4 - p^2$  for  $p^2 \leq \eta^2/4$ , and  $m^2(p^2) = 0$  otherwise. There is no mass-shell, i.e.  $p^2 + m^2(p^2) \neq 0$  for any  $p^2$ , and there is quark confinement. The above solution holds at  $T = 0$  and at  $T > 0$  with  $p^2$  replaced by  $p_n^2 = \omega_n^2 + \vec{p}^2$ . Thus for  $T > T_c = \eta/(2\pi)$  there is chiral restoration. Results from this model at finite  $T, \mu$  have been obtained for quark thermodynamics outside the phase boundary of chiral restoration as governed by the quark propagator [11]. The behavior of the masses of both the  $\pi$  and  $\rho$  modes for  $T < T_c$  (and also for chemical potential dependence for  $\mu < \mu_c$ ) have also been obtained [12].

With Eq. (41), the BSE given in Eq. (2) becomes

$$\lambda(P^2)\Gamma(q; P) = -\frac{\eta^2}{4} \gamma_\mu S(q_+) \Gamma(q; P) S(q_-) \gamma_\mu, \quad (43)$$

and solutions are possible if  $q$  is fixed by  $P$ . At  $T > 0$ , the solution that connects smoothly to the  $T = 0$  solution has the normally independent variable  $q_n = (\omega_n, \vec{q})$  restricted to  $q_n \rightarrow (\omega_0, \vec{0})$ . To obtain spatial meson modes to compare with the separable model results, we again set  $P = (0, \vec{P})$ . As discussed in Ref. [12] for  $T < T_c = \eta/(2\pi)$ , simple results obtain for the pseudoscalar and vector spatial modes. One finds  $\lambda_\pi(0) = 1$  for the chiral limit  $\pi$ ; thus  $M_\pi = 0$ . For the vector meson one finds that  $\lambda_\rho^T(-\eta^2/2) = 1$ ; thus  $M_\rho^T = \eta/\sqrt{2}$ . These are the correct  $T = 0$  results of the model. They hold over the finite temperature domain for which the quark mass function appropriate to the propagators occurring in the BS Eq. (43) is nonzero. For the equation appropriate to a meson of mass  $M$ , the relevant domain for the present model is  $\eta^2 - 4s > 0$  where  $s = \pi^2 T^2 - M^2/4$ . For  $M_\pi = 0$ , this temperature domain corresponds to that for which the model DSE generates a dynamical quark mass function in accord with the Goldstone theorem. For larger  $M$ , this temperature domain will be larger. The vector result  $M_\rho = \eta/\sqrt{2}$  holds for  $T < \sqrt{3}/2T_c$ . We fix the single parameter  $\eta = 1.107$  GeV, so that  $M_\rho = 0.783$  GeV. This produces  $T_c = 0.176$  GeV. The constant masses in their respective temperature domains are displayed in Fig. 9.

Beyond these two temperature domains, one finds

$$\lambda_\pi(\vec{P}^2) = \eta^2 s_- \sigma_A^2(s_+), \quad (44)$$

where  $s_\pm = \pi^2 T^2 \pm \vec{P}^2/4$ , and

$$\lambda_\rho^T(\vec{P}^2) = \frac{1}{2} \lambda_\pi(\vec{P}^2). \quad (45)$$

In general both functions  $\lambda(-M^2)$  decrease with increasing  $T$  and increase with increasing  $M$ . Thus the spatial eigenmode condition  $\lambda(-M^2) = 1$  will tend to maintain  $M_\rho^T(T) > M_\pi(T)$  while both masses rise with  $T$ . The behavior at such high temperatures

is indicated in Fig. 9. The temperature at which  $M_\rho^T = 2M_\pi$  here is  $1.33 T_c$ . Considering that the chiral limit is employed in Fig. 9 for simplicity, while the rank-1 separable model behavior in Fig. 8 corresponds to a physical current quark mass (and hence  $\pi$  mass), the qualitative behavior of both models is essentially the same. The main difference is that the mass defect  $\Delta(T) = 2\pi T - M(T)$  is significantly larger in the ID model and is not evidently decreasing for the range of  $T$  shown. As confirmation, the leading large  $T$  behavior of  $M_\rho^T(T)$  can be found from Eqs. (44) and (45) with the help of Eq. (42) and is

$$M_\rho^{T^2}(T) \rightarrow (2\pi T)^2 \left(1 - \frac{\eta}{\pi T} \dots\right). \quad (46)$$

Hence the asymptotic spatial mass defect of the transverse  $\rho$  mode has the value  $\Delta_\rho(T) \rightarrow \eta$ . Only about half this value has been reached at the maximum temperature shown in Fig. 9.

In Fig. 10 the  $\pi$  and transverse  $\rho$  spatial masses at  $T > T_c$  from both the rank-1 separable model and the ID model are presented in comparison with lattice QCD simulations of spatial screening masses [28]. The solid horizontal line marks  $2\pi$  while the lower horizontal dot-dashed line represents the lattice free limit corrected [28] for the lattice time extent  $N_t$ . From Fig. 10 it is evident that for the  $\pi$  at  $T > T_c$ , the spatial or screening mass defect  $\Delta = 2\pi T - M(T)$  is decreasing more rapidly above  $T_c$  in the rank-1 separable model than is evident from the lattice simulations. We attribute this to the fact that the quark vector self-energy amplitudes  $A(p, T) - 1$  and  $C(p, T) - 1$  are zero in the rank-1 separable model. In contrast, the ID model, which has significant strength in those amplitudes, produces a mass defect for both  $\pi$  and  $\rho$  that is much stronger; it is in fact too strong when compared with the lattice QCD simulations. This persistent self-interaction well above  $T_c$ , which slows the approach to free behavior such as Stefan-Boltzmann thermodynamics [11], may well be what is signaled by the lattice QCD data in Fig. 10.

## V. DISCUSSION

We have explored a simple separable interaction model within the rainbow-ladder truncation of the quark Dyson-Schwinger equation and the  $\bar{q}q$  Bethe-Salpeter equation for finite temperature below and above  $T_c$ . With parameters fitted to  $T = 0$  properties related to the  $\pi$  and  $\rho$  mesons, the model possesses dynamical chiral symmetry breaking and quark confinement. The  $T > 0$  extension via the Matsubara formalism produces temperatures for deconfinement  $T_d$  and chiral restoration  $T_c$  that are very similar and in the range 100-150 MeV. The model is then used to study the  $T$ -evolution of the  $\pi$  and  $\rho$   $\bar{q}q$  states in the presence of the deconfinement and chiral restoration mechanisms. The degree to which the model respects the axial vector Ward-Takahashi relation is evaluated in terms of the exact pion mass relation and the related GMOR relation. The widths for the electromagnetic decay  $\rho^0 \rightarrow e^+e^-$  and the strong decay  $\rho \rightarrow \pi\pi$  are also studied. Finally, the high  $T$  behavior of the spatial masses is compared to that of spatial screening masses from lattice QCD simulations [28].

The masses  $M_\pi(T)$ ,  $M_\rho^T(T)$  and  $M_\rho^L(T)$  are found to be almost  $T$ -independent below  $T_c$  followed by a strong increase. This behavior is characteristic of lattice QCD simulations [27,28] and DSE studies [12,19]. We find that the  $\rho \rightarrow \pi\pi$  strong decay width decreases

with  $T$  and by  $T_c$  it has been reduced by 50%. It becomes phase-space blocked at about 25 MeV above  $T_c$ . (The same phase-space blocking happens essentially at  $T_c$  for the strong  $\pi\pi$  decay of the scalar-isoscalar partner of the pion [19].) Here the transverse  $\rho$  mode is left with a narrow total width typical of electromagnetic decay. On the basis of the present study, one would expect the mass of the pseudoscalar  $K$  correlation to rise with  $T$  in a similar fashion to  $M_\pi$ , while the mass of the vector  $\phi$  mode should rise like the  $\rho$ . This suggests that the vector modes  $\rho$ ,  $K^*$  and  $\phi$  tend to be trapped with their relatively long electroweak lifetimes and with significantly increased masses for a domain of high temperatures above the transition. Between 0.5-1.0  $T_c$ , the transition probability connecting vector correlations with pairs of pseudoscalars would be clearly reduced. This suggests that within the gas of pions and other pseudoscalars that dominate the hot hadronic product from heavy-ion collisions, the role of vector meson correlations in producing the dilepton spectra could be significantly less than conventional expectations. The present findings follow from the response of the quark-gluon content of the mesons to the heat bath. A different phenomena is the coupling of the meson modes to the many-hadron environment which introduces a collisional broadening effect [2]. An approach that incorporates both phenomena is clearly called for.

Only the spatial or screening  $\bar{q}q$  masses have been investigated within this model. The temporal masses (sometimes called dynamical or pole masses) will in general be different. Lattice simulations indicate that spatial masses become much larger than the temporal masses above  $T_c$  [30]. A Nambu–Jona-Lasinio model study [29] found that they are significantly different only in the range  $150 \text{ MeV} < T < 350 \text{ MeV}$ . A possible explanation for this discrepancy lies in our finding that the mass defect  $\Delta = 2\pi T - M(T)$  at high  $T$  is significantly influenced by residual non-perturbative interaction effects in the Dirac vector amplitude  $A(P^2) - 1$  of the quark self-energy. Such a term is not present in the Nambu Jona–Lasinio model.

The Gaussian form factor employed here can simulate only the gross features of the infrared behavior of the dressed quark self-energy amplitudes that is evident in more realistic  $T = 0$  studies. Detailed results from this type of model could presumably be improved via use of different form factors. Nevertheless, the qualitative behavior of the results for the spatial masses of  $\rho$  and  $\pi$  modes indicated in this present work are expected to remain. The only  $T$ -dependence of the effective quark-quark interaction implemented by the present separable model is that generated by the Matsubara frequencies that enter through the momentum dependence. The strength and range parameters have been kept  $T$ -independent and no attempt has been made to introduce explicit  $T$ -dependent characteristics such as a Debye mass. Such considerations are more appropriately handled in approaches that have a better connection to a perturbative gluon propagator [19].

The simplicity of a separable representation of the effective quark-quark interaction of the type studied here might be of advantage in the consideration of pion loop effects and bulk thermodynamic properties of the hadron-quark matter phase transitions. Initial thermodynamic considerations have been reported recently [18].

## ACKNOWLEDGMENTS

We acknowledge fruitful interactions and conversations with B. Van den Bossche, M. Buballa, C.D. Roberts, and S. Schmidt. The work of G.B. and Y.L.K. has been supported by the Max-Planck-Gesellschaft and by the DFG Graduiertenkolleg “Stark korrelierte Vielteilchensysteme”. D.B. and G.B. gratefully acknowledge financial support by the Deutscher Akademischer Austauschdienst (DAAD) for visits to the Center for Nuclear Research at Kent State University where part of this work was conducted. Y.L.K. also acknowledges the Russian Fund for Fundamental Research, under contract number 97-01-01040, and the support of the Heisenberg-Landau program. P.C.T. and P.M. acknowledge support by the National Science Foundation under Grant Nos. INT-9603385 and PHY97-22429 and the hospitality of the University of Rostock where part of this work was conducted during several visits.

## REFERENCES

- [1] *Quark Matter '99*, Eds. L. Riccati, M. Masera, and E. Vercellin, Nucl. Phys. **A 661** (1999).
- [2] R. Rapp and J. Wambach, “Chiral symmetry restoration and dileptons in relativistic heavy-ion collisions”, Adv. Nucl. Phys. in press, hep-ph/9909229; R. Rapp and C. Gale, Phys. Rev. **C 60**, 024903 (1999).
- [3] C. D. Roberts and A. G. Williams, Prog. Part. Nucl. Phys. **33**, 477 (1994); C. D. Roberts, Fiz. Élem. Chastits At. Yadra **30**, 537 (1999) (Phys. Part. Nucl. **30**, 223 (1999)).
- [4] P. Maris and C. D. Roberts, Phys. Rev. **C56**, 3369 (1997).
- [5] P. Maris and P. C. Tandy, Phys. Rev. **C60**, 055214 (1999).
- [6] P. C. Tandy, Prog. Part. Nucl. Phys. **39**, 117 (1997).
- [7] P. C. Tandy, Fizika **B8**, 295 (1999).
- [8] A. Bender, D. Blaschke, Yu. L. Kalinovsky, C. D. Roberts, Phys. Rev. Lett. **77**, 3724 (1996) .
- [9] A. Bender, G. I. Poulis, C. D. Roberts, S. Schmidt and A. W. Thomas, Phys. Lett. **B431**, 263 (1998).
- [10] H. J. Munczek and A. M. Nemirovsky, Phys. Rev. **D28**, 181 (1983).
- [11] D. Blaschke, C. D. Roberts, S. Schmidt, Phys. Lett. **B 425**, 232 (1998).
- [12] P. Maris, C. D. Roberts, S. Schmidt, Phys. Rev. **C 57**, R2821 (1998).
- [13] J. C. R. Bloch, C. D. Roberts and S. M. Schmidt, Phys. Rev. **C 60**, 065208 (1999).
- [14] H. Ito, W. Buck and F. Gross, Phys. Rev. **C 43**, 2483 (1991); Phys. Rev. **C 45**, 1918 (1992); M. Buballa and S. Krewald, Phys. Lett. **B 294**, 19 (1992); R. S. Plant and M. C. Birse, Nucl. Phys. **A 628**, 607 (1998).
- [15] S. Schmidt, D. Blaschke, and Yu. L. Kalinovsky, Phys. Rev. **C 50**, 435 (1994).
- [16] C. J. Burden, Lu Qian, C. D. Roberts, P. C. Tandy and M. J. Thomson, Phys. Rev. **C 55**, 2649 (1997).
- [17] D. Blaschke, Yu.L. Kalinovsky and P. Tandy, in: Proc. of the XI Int. Conf. on *Problems of Quantum Field Theory*, Dubna, July 13-17, p.454, 1998; hep-ph/9811476.
- [18] D. Blaschke and P. C. Tandy, in *Understanding Deconfinement in QCD*, Eds. D. Blaschke, F. Karsch and C. D. Roberts, (World Scientific, Singapore), p. 218, 1999.
- [19] P. Maris, C. D. Roberts, S. M. Schmidt and P. C. Tandy, “*T*-dependence of pseudoscalar and scalar correlations”, preprint, KSUCNR-102-00, (2000), nucl-th/0001064.
- [20] C. D. Roberts, A.G. Williams and G. Krein, Int. J. Mod. Phys. **A 7**, 5607 (1992).
- [21] P. Maris, C. D. Roberts and P. C. Tandy, Phys. Lett. **B 420**, 267 (1998).
- [22] M. A. Ivanov, Yu. L. Kalinovsky and C. D. Roberts, Phys. Rev. **D 60**, 034018 (1999).
- [23] L. C. L Hollenberg, C. D. Roberts and B. H. J. McKellar, Phys. Rev. **C 46**, 2057 (1992); D. B. Leinweber and T. D. Cohen, Phys. Rev. **D 49**, 3512 (1994); K. L. Mitchell and P. C. Tandy, Phys. Rev. **C55**, 1477 (1995); M. A. Pichowsky, S. Walawalkar, and S. Capstick, Phys. Rev. **D 60**, 054030 (1999).
- [24] D. Blaschke, A. Höll, C. D. Roberts and S. Schmidt, Phys. Rev. **C 58**, 1758 (1998); A. Höll, P. Maris and C. D. Roberts, Phys. Rev. **C 59**, 1751 (1999).
- [25] S. Schmidt, D. Blaschke, and Yu. L. Kalinovsky, Z. Phys. **C 66**, 485 (1995).
- [26] H.-J. Schulze and D. Blaschke, Phys. Lett. **B 386**, 429 (1996).

- [27] F. Karsch and E. Laermann, Rep. Prog. Phys. **56**, 1347 (1993); E. Laermann, Fiz. Élem. Chastits At. Yadra **30**, 720 (1999) (Phys. Part. Nucl. **30**, 304 (1999)).
- [28] A. Gocksch, Phys. Rev. Lett. **67**, 1701 (1991); K. Born et al., Phys. Rev. Lett. **67**, 302 (1991).
- [29] W. Florkowski and B. L. Friman, Acta. Phys. Pol. **B25**, 49 (1994).
- [30] QCD-TARO Collaboration, "Mesons above the Deconfining transition", preprint hep-lat/9901017.

## FIGURES

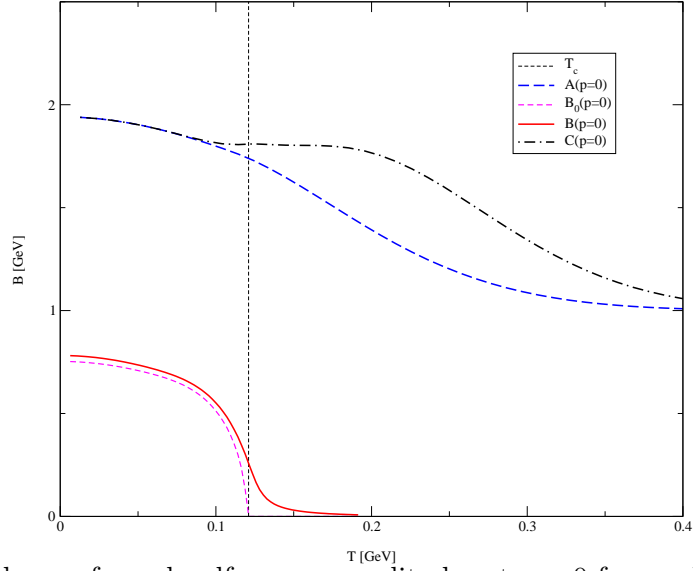


FIG. 1.  $T$ -dependence of quark self-energy amplitudes at  $p = 0$  from solution of the DSE.

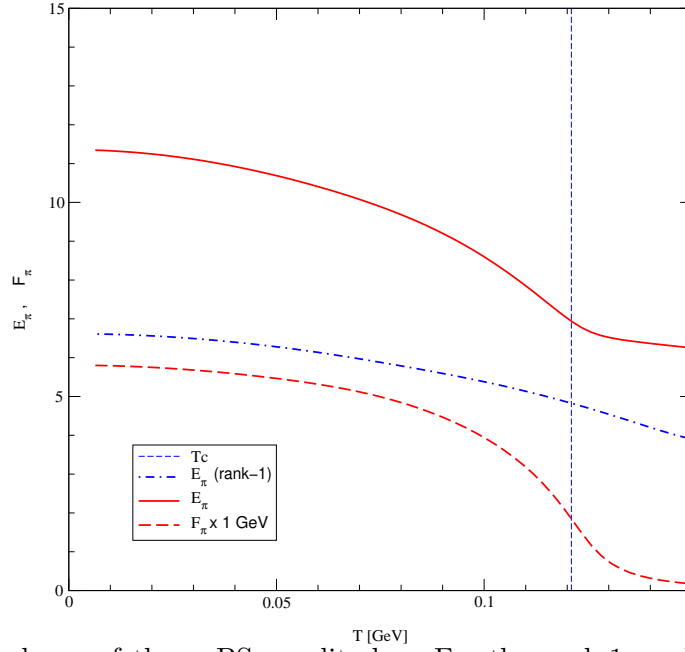


FIG. 2.  $T$ -dependence of the  $\pi$  BS amplitudes. For the rank-1 model, only the dominant amplitude  $E_\pi$  is used; for the rank-2 model, both contributing amplitudes  $E_\pi$  and  $F_\pi$  are used.

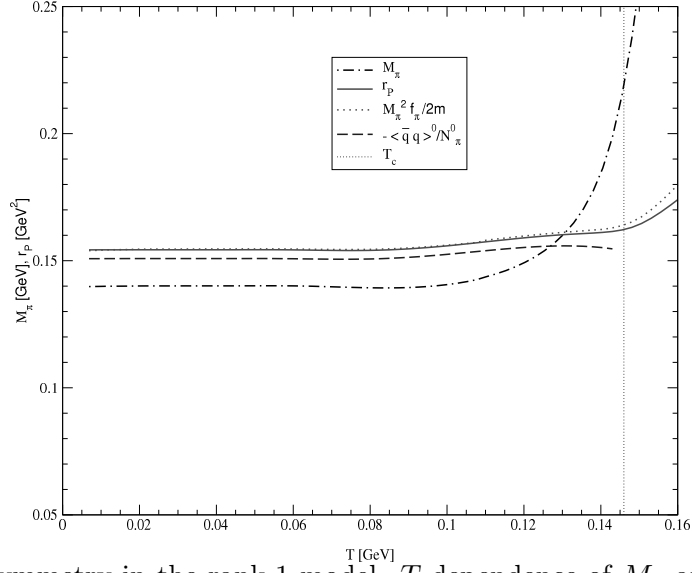


FIG. 3. Chiral symmetry in the rank-1 model.  $T$ -dependence of  $M_\pi$  and quantities involved in the exact pion mass relation and the GMOR relation.

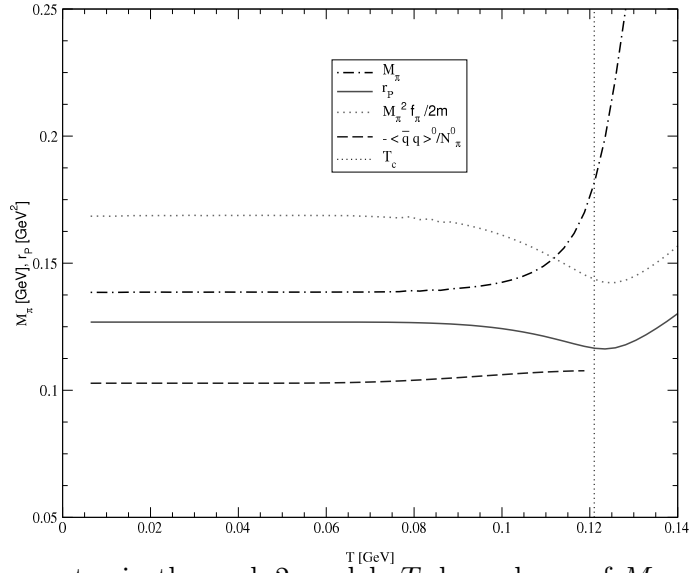


FIG. 4. Chiral symmetry in the rank-2 model.  $T$ -dependence of  $M_\pi$  and quantities involved in the exact pion mass relation and the GMOR relation.

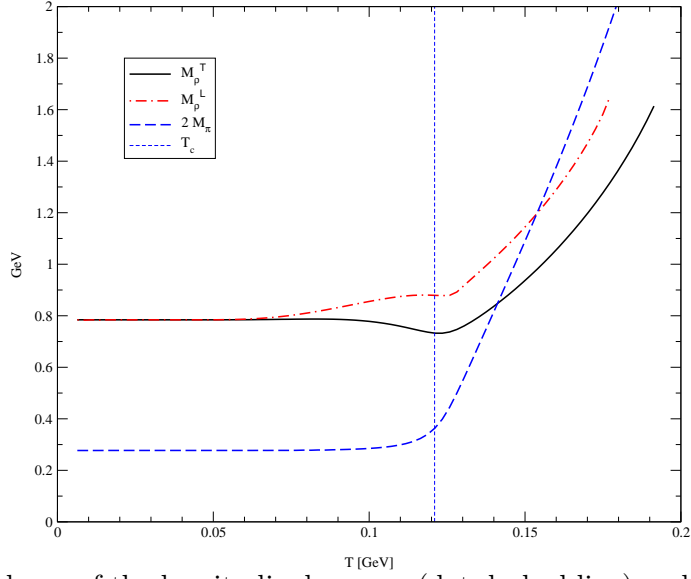


FIG. 5.  $T$ -dependence of the longitudinal  $\rho$  mass (dot-dashed line) and the transverse  $\rho$  mass (solid line). Also shown is  $2M_\pi$  indicating that the strong decay channel becomes inaccessible within 20-30 MeV beyond  $T_c$ . Results are from the rank-2 model.

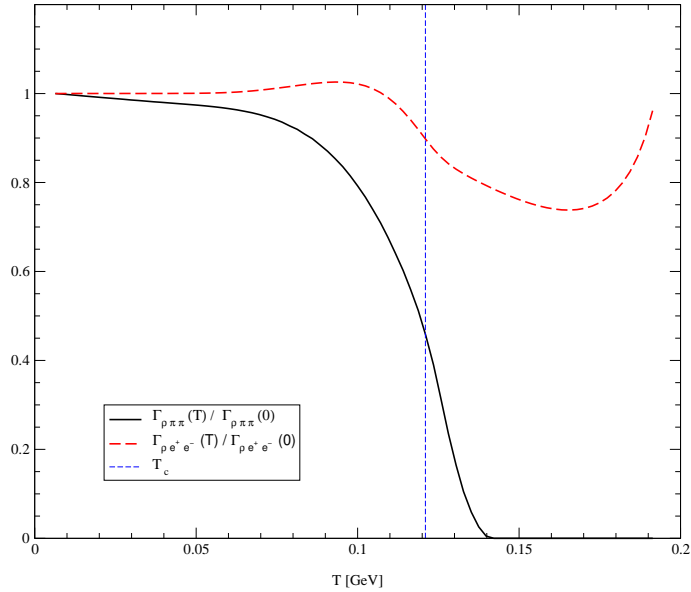


FIG. 6.  $T$ -dependence of the transverse  $\rho$  partial widths due to electromagnetic  $e^+e^-$  decay (dashed line) and strong  $\pi\pi$  decay (solid line). Only the electromagnetic decay is available beyond 142 MeV. Results are from the rank-2 model.

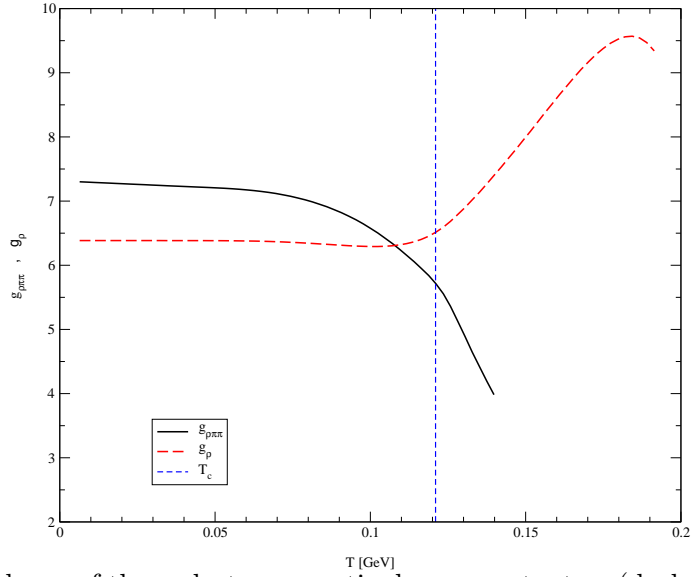


FIG. 7.  $T$ -dependence of the  $\rho$  electromagnetic decay constant  $g_\rho$  (dashed line) and the strong coupling constant  $g_{\rho\pi\pi}$  (solid line) corresponding to the widths shown in Fig. 6.

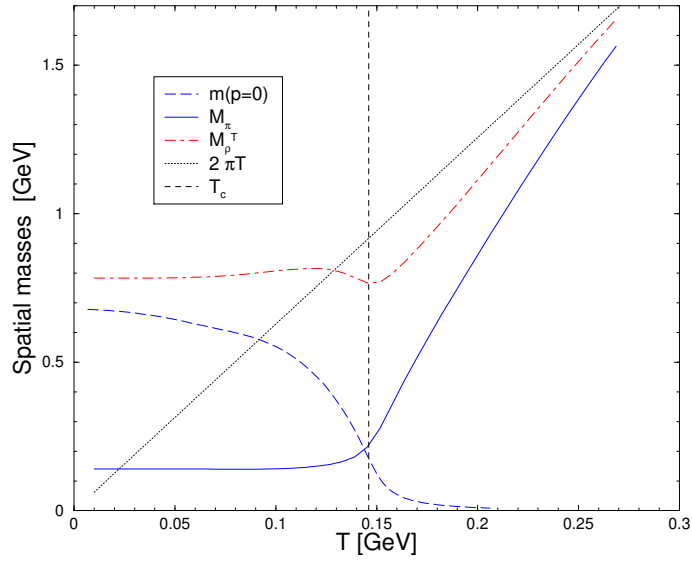


FIG. 8. High  $T$  behavior of the spatial masses of the  $\pi$  and transverse  $\rho$  modes from the rank-1 separable model.

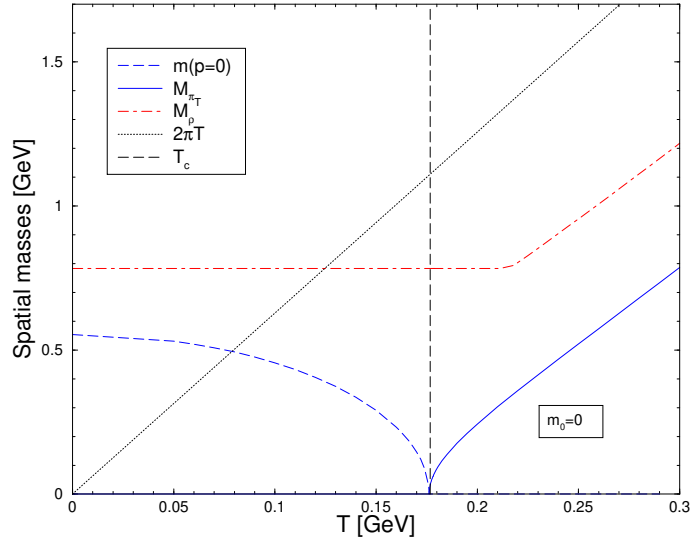


FIG. 9. Spatial masses of the  $\pi$  and transverse  $\rho$  modes from the semi-analytic infrared-dominant (ID) model in the chiral limit.

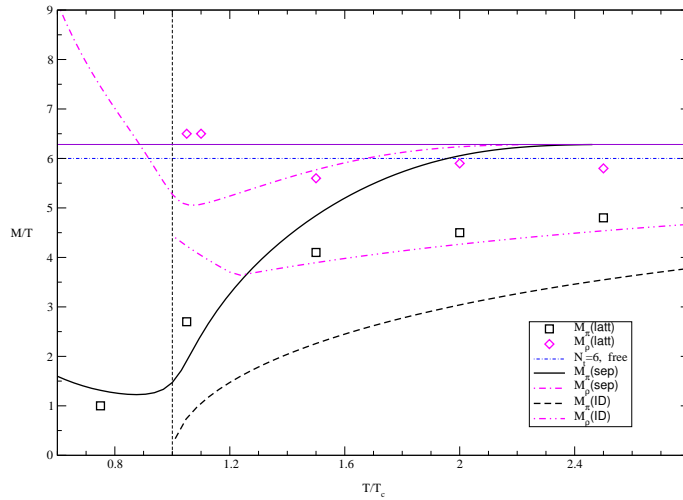


FIG. 10. Spatial masses from the rank-1 separable model (sep) and the infrared dominant model (ID) compared to spatial screening masses from lattice QCD simulations (latt) taken from [28].

TABLES

	Experiment	rank-1	rank-2
$-\langle\bar{q}q\rangle^0$	$(0.236 \text{ GeV})^3$	0.248	0.203
$m_0$	5 - 10 MeV	6.6	5.3
$m(p^2 = 0)$	$\sim 0.350 \text{ GeV}$	0.685	0.405
$M_\pi$	0.1385 GeV	0.140	0.139
$f_\pi$	0.093 GeV	0.104	0.093
$N_\pi/f_\pi$	1.0	0.987	0.740
$M_{\rho/\omega}$	0.783 GeV	0.783	0.784
$g_\rho$	5.03	5.04	6.38
$(f_\rho)$	$(0.216 \text{ GeV})$	$(0.220)$	$(0.174)$
$\Gamma_{\rho^0 \rightarrow e^+e^-}$	6.77 keV	6.88	4.29
$g_{\rho\pi\pi}$	6.05	5.71	7.22
$\Gamma_{\rho \rightarrow \pi\pi}$	151 MeV	137	221
Parameters			
$D_0\Lambda_0^2$		128.0	260.0
$\Lambda_0$		0.687 GeV	0.638 GeV
$D_1\Lambda_1^4$		0	130.0
$\Lambda_1/\Lambda_0$			1.21

TABLE I. Calculated properties at  $T = 0$  for the  $u/d$  quark mesons  $\pi$  and  $\rho$  along with related quark properties and parameters for the rank-1 and rank-2 separable models. The quoted experimental values for both the quark condensate and the current  $u/d$  quark mass  $m_0$  are appropriate to a renormalization scale of  $\mu \sim 1 \text{ GeV}$ . The scale for the model calculations may be considered to be set by  $\Lambda_0$ .